Published in Hydrogeology Journal 17, issue 3, 589-600, 2009
which should be used for any reference to this work

Understanding diagnostic plots for well-test interpretation

Philippe Renard · Damian Glenz · Miguel Mejias

Keywords Hydraulic testing · Conceptual models · Hydraulic properties · Analytical solutions

Abstract In well-test analysis, a diagnostic plot is a scatter plot of both drawdown and its logarithmic derivative versus time. It is usually plotted in log–log scale. The main advantages and limitations of the method are reviewed with the help of three hydrogeological field examples. Guidelines are provided for the selection of an appropriate conceptual model from a qualitative analysis of the log-derivative. It is shown how the noise on the drawdown measurements is amplified by the calculation of the derivative and it is proposed to sample the signal in order to minimize this effect. When the discharge rates are varying, or when recovery data have to be interpreted, the diagnostic plot can be used, provided that the data are pre-processed by a deconvolution technique. The effect of time shift errors is also discussed. All these examples show that diagnostic plots have some limitations but they are extremely helpful because they provide a unified approach for well-test interpretation and are applicable in a wide range of situations.

Introduction

Among the techniques used to characterize the hydraulic properties of aquifers, well testing is one of the most commonly applied. It involves imposing a perturbation such as pumping in a well and measuring the response of the aquifer, for example in terms of head variations. Those data are then interpreted with the help of analytical or numerical models in order to infer the hydraulic properties of the aquifer.

In that framework, a diagnostic plot (Bourdet et al. 1983) is a simultaneous plot of the drawdown and the logarithmic derivative $(\partial s/\partial \ln t = t\partial s/\partial t)$ of the drawdown as a function of time in log–log scale. This plot is used to facilitate the identification of an appropriate conceptual model best suited to interpret the data.

The idea of using the logarithmic derivative in well-test interpretation is attributed to Chow (1952). He demonstrated that the transmissivity of an ideal confined aquifer is proportional to the ratio of the pumping rate by the logarithmic derivative of the drawdown at late time. He then developed a graphical technique to apply this principle, but this finding had a limited impact until the work of Bourdet and his colleagues (Bourdet et al. 1989; Bourdet et al. 1983). They generalized the idea and analyzed the behaviour of the log-derivative for a large number of classical models of flow around a pumping well. Doing so they showed that the joint use of the drawdown and its log-derivative within a unique plot had many advantages:

- The logarithmic derivative is highly sensitive to subtle variations in the shape of the drawdown curve. It allows detecting behaviours that are difficult to observe on the drawdown curve alone.
- The analysis of the diagnostic plot of a data set facilitates the selection of a conceptual model.
- For certain models, the values of the derivative can directly be used to estimate rapidly the parameters of the model.

Overall, one of the main advantages of the diagnostic plots is that they offer a unified methodology to interpret pumping test data. Indeed, between the work of Theis in 1935 and the work of Bourdet in 1983 (Bourdet et al. 1983), a wide range of models has been developed (bounded aquifers, double porosity, horizontal fracture, vertical fracture, unconfined aquifer, etc.). Many of these models required specific plots and interpretation techniques (see for example Kruseman and de Ridder 1994, for an excellent synthesis).

Using the diagnostic plot allows for the replacement of all these specialized tools with a simple and unique approach that can be applied to any new solutions, as it has been done

P. Renard (✉) · D. Glenz
Centre for Hydrogeology,
University of Neuchâtel,
11 Rue Emile Argand, CP-158, 2009, Neuchâtel, Switzerland
e-mail: philippe.renard@unine.ch

D. Glenz
e-mail: damien.glenz@unine.ch

M. Mejias
Geological Survey of Spain (IGME),
Ríos Rosas 23, 28003, Madrid, Spain

M. Mejias
e-mail: m.mejias@igme.es

for example by Hamm and Bideaux (1996), Delay et al. (2004), or Beauheim et al. (2004). Today most of the theoretical works related to well testing include diagnostic plots both in hydrogeology and the petroleum industry.

However, the situation is different in these two fields of application (Renard 2005a). The technique has become a standard in petroleum engineering over the last 20 years. It has been popularized by a series of papers and books (Bourdet 2002; Bourdet et al. 1989; Bourdet et al. 1983; Ehlig-Economides et al. 1994b; Horne 1995; Horne 1994; Ramey 1992). In hydrogeology, the technique is used routinely only in some specific or highly technical projects such as the safety analysis of nuclear waste repositories. Therefore, even if the concept has already been introduced and described in hydrogeological journals (e.g. Spane and Wurstner 1993), only a minority of hydrogeologists are using diagnostic plots and the technique is not taught in specialized hydrogeology textbooks.

This is why there is still a need to promote the use of this technique in hydrogeology to reach a large part of the profession by explaining how the technique works and how it can be used in practice. The technique presents some difficulties and limitations that have been highlighted by the detractors of the approach. These difficulties are often real and must be discussed as well in order to understand what can be done and what cannot be done. In addition, most commercial and open-source pumping-test interpretation software are now providing the option to compute the logarithmic derivative and therefore many users would benefit from a better understanding of this tool.

The objective of this report is therefore to provide an introduction to the diagnostic plots for the practitioners. The main advantages and limitations of this tool are discussed and illustrated through the study of a few field examples. Along the presentation, some theoretical points are discussed to explain how the method works and to facilitate its understanding.

Before discussing the examples and the method, it is important to emphasize that diagnostic plots are calculated on drawdowns. Therefore, the original data must have been preprocessed in order to remove the head variations independent of pumping (both natural or induced by nearby pumping operations). For example, tools are available to remove barometric or earth tide effects (Toll and Rasmussen 2007). This is a standard procedure (Dawson and Istok 1991) that needs to be applied whether one uses diagnostic plots or not, therefore this aspect will not be discussed further here.

An introductory example

A pumping test has been conducted in a confined aquifer for 8 h and 20 min at a steady pumping rate of 50 m^3/h. The drawdown data, measured in an observation well located 251 m away from the pumping well, are reported by Fetter (2001, p. 172).

To analyse this data set with a diagnostic plot, the procedure starts by calculating the log-derivative of the data, and plotting simultaneously the drawdown and the log derivative. The corresponding diagnostic plot is illustrated in Fig. 1. The circles represent the original drawdown data and the crosses the log-derivative. The plot shows that the derivative is larger than the drawdown at early time and then it becomes smaller than the drawdown and tends to stabilize. At late time, the derivative slightly oscillates.

In order to identify which model can be used to interpret these data, one needs to compare the diagnostic plot with a set of typical diagnostic plots such as those shown in Fig. 2; note that Fig. 2 will be presented in detail in a later section. For the moment, it will be used as a catalogue of typical behaviours.

Neglecting the oscillations of the derivative at late time, the comparison between Figs. 1 and 2 shows that the overall behaviour resembles very much what is depicted in Fig. 2a in log–log scale. There is no major increase or decrease of the derivative at late time, as can be seen for example in Fig. 2h,d, or e. At early time, the derivative either does not follow the drawdown curve as it does in Fig. 2f, or it does not remain systematically smaller than the drawdown curve as in Fig. 2g. Additionally, there is not any major hole in the derivative like in Fig. 2b; therefore, one can conclude that the model that best represents the data is the Theis model corresponding to Fig. 2a.

Once the model (or the set of possible models) has been identified, the procedure consists of estimating the parameters of the model that allow for the best reproduction of the data. This is usually done with least-squares procedures and there are many examples of these both in the petroleum and hydrogeology literature (Bardsley et al. 1985; Horne 1994). What is important to highlight is that when diagnostic plots are used, it is interesting to display

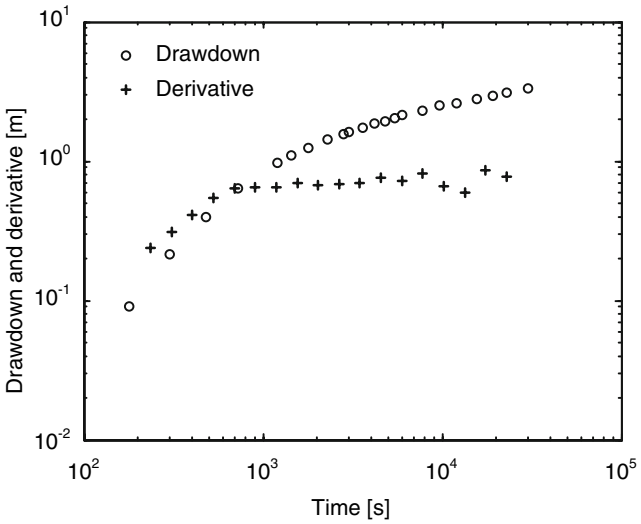

Fig. 1 Diagnostic plot of the Fetter (2001) drawdown data. The *vertical axis* represents both the drawdown and the logarithmic derivative

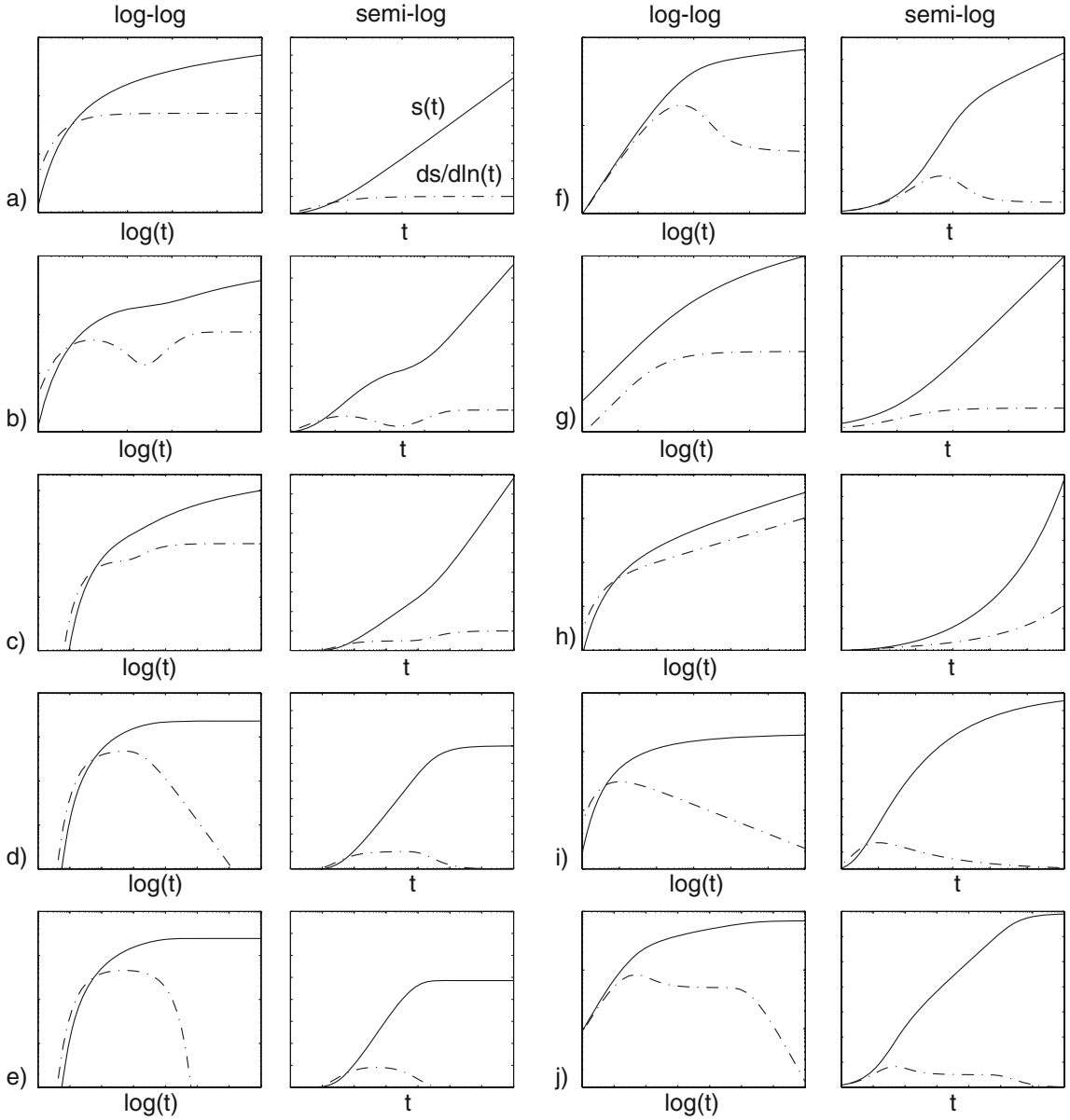

Fig. 2 Most typical diagnostic plots encountered in hydrogeology: **a** Theis model: infinite two-dimensional confined aquifer; **b** double porosity or unconfined aquifer; **c** infinite linear no-flow boundary; **d** infinite linear constant head boundary; **e** leaky aquifer; **f** well-bore storage and skin effect; **g** infinite conductivity vertical fracture.; **h** general radial flow—non-integer flow dimension smaller than 2; **i** general radial flow model—non-integer flow dimension larger than 2; **j** combined effect of well bore storage and infinite linear constant head boundary (modified from Renard 2005b)

(e.g. Fig. 3) the diagnostic plot of the data with the diagnostic plot of the fitted model in the same graph. One can then very rapidly check visually if the fit is acceptable and if the model derivative reproduces the observed data.

Infinite acting radial flow (IARF)

Figure 3 shows an important characteristic of the Theis model: the logarithmic derivative of the model stabilizes at late time. This is due to the fact that the Theis (1935) solutions tend asymptotically toward the Cooper and Jacob (1946) asymptote:

$$\lim_{t\to\infty} s(t) = \frac{Q}{4\pi T} \ln\left(\frac{2.25tT}{r^2 S}\right) \tag{1}$$

where s [m] represents the drawdown, t [s] the time since the pumping started, Q [m^3/s] the pumping rate, T [m^2/s] the transmissivity, r [m] the distance between the pumping well and the observation well, and S [–] the storativity. Note that ln represents the natural logarithm. Computing

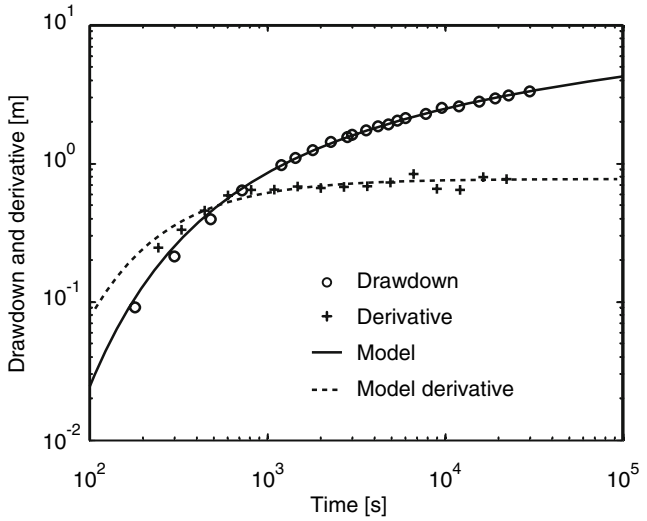

Fig. 3 Example of the diagnostic plot of the Fetter (2001) data superimposed with a fitted Theis model. One can observe that the fit is rather good and that the model reproduces well the main features of the drawdown data and its derivative

the logarithmic derivative of the Cooper-Jacob asymptote shows that it is a constant value:

$$\frac{\partial s}{\partial \ln t} = t\frac{\partial s}{\partial t} = t\frac{Q}{4\pi T}\frac{1}{t} = \frac{Q}{4\pi T} \tag{2}$$

Therefore, when the Theis solution reaches its Cooper-Jacob asymptote, the logarithmic derivative becomes constant. Note that Eq. (2) was published by Chow (1952).

When interpreting a field data set, observing that the derivative increases or decreases during a certain time period indicates that the Cooper-Jacob approximation cannot be applied during that time period. If the derivative is constant during a certain time period, then it is a graphical indication that the response of the aquifer is following a Cooper-Jacob straight line. Going a step further, it means that the stabilization of the logarithmic derivative is an indication that the assumptions underlying the Theis model, i.e. a two-dimensional infinite acting radial flow (IARF), are most probably valid. In other words, when the derivative is constant the flow around the well can be described by a set of streamlines converging to a circular cylinder. It is therefore common practice when analyzing a data set to look for the periods in which such stabilization occurs and to name them IARF periods.

Because one of the main aims of conducting pumping test is to obtain reliable estimates of transmissivity, it is recommended when conducting a test to stop it only when the data show at least 1–1.5 log-cycles during which the derivative is constant. This ensures that a reliable estimate of the transmissivity can be obtained with the straight-line analysis method. In those cases, Eq. (2) provides a way to estimate rapidly the transmissivity. One need only note the value of d of the log-derivative on the diagnostic plot, to estimate the transmissivity:

$$T = \frac{Q}{4\pi d} \tag{3}$$

For example in Fig. 1, the mean value of the log-derivative is around 0.8 m. Then the transmissivity can be estimated with:

$$T = \frac{1.39\ 10^{-2}\left[m^3/s\right]}{4\pi \times 0.8[m]} = 1.4\ 10^{-3}\left[m^2/s\right] \tag{4}$$

which compares well with the value of 1.5 10^{-3} m^2/s that was obtained by Fetter (2001) using type curve matching.

Noise in the derivative

Why were the oscillations that affect the late time derivative neglected during the interpretation of Fig. 1? One has to remember that the logarithmic derivative is calculated from the drawdown data. By definition, the logarithmic derivative is equal to

$$\frac{\partial s}{\partial \ln t} = t\frac{\partial s}{\partial t} \tag{5}$$

When data collected from the field are used, the logarithmic derivative has to be evaluated numerically from a discrete series of n drawdown s_i and time t_i values. These n couples of values are the circles represented in Fig. 1. Then, there are many ways to compute the log derivative.

The most simple is the following:

$$\left.\frac{\partial s}{\partial \ln t}\right|_{t_m} = \frac{s_i - s_{i-1}}{\ln(t_i) - \ln(t_{i-1})} \tag{6}$$

This approximation is associated with the time t_m corresponding to the centre of the time interval (calculated as the arithmetic mean $t_m = (t_i + t_{i-1})/2$ or geometric mean $t_m = \sqrt{t_i t_{i-1}}$ of the two successive time values). Another possibility is to compute the slope between two successive data points, and to multiply it by the time corresponding to the centre of the interval.

$$\left.\frac{\partial s}{\partial \ln t}\right|_{t_m} \approx \left(\frac{t_i + t_{i-1}}{2}\right)\left(\frac{s_i - s_{i-1}}{t_i + t_{i-1}}\right) \tag{7}$$

When frequent measurements are made and when the data are very accurate, the approximations written in Eqs. (6) or (7) provide a very good estimation of the log-derivative. However, when the time variation between two measurements is rather large and/or when the drawdown measurements are affected by measurement uncertainties (due to the resolution and/or accuracy of the

measurement device and data acquisition system used) that are on the order of magnitude of the drawdown variation between two successive measurements, then the calculated derivative can be extremely noisy.

For example, Fig. 4a shows the diagnostic plots of a data set collected manually in an observation well during a pumping test in a coastal aquifer in Tunisia (G. de Marsily, University of Paris 6, personal communication, 1995). The derivative was calculated with Eq. (3). In that case, the noise masks most of the signal and makes the interpretation difficult.

In order to minimize these artefacts, more robust numerical differentiation schemes have been proposed. Bourdet et al. (1989), Spane and Wurstner (1993), Horne (1995), or Veneruso and Spath (2006) discuss and present different techniques such as smoothing the data prior to the computation of the derivative, or smoothing the derivative.

In hydrogeology, when the number of data points can be rather limited and irregularly spaced in time because of manual sampling, a robust and simple solution involves resampling (with a spline interpolation) the signal at a fixed number of time intervals regularly spaced in a logarithmic scale. The derivative is then computed with Eq. (3) on the resampled signal. Using 20–30 resampling points is usually sufficient to get a good estimation of the general shape of the derivative as it is illustrated on Fig. 4b.

Comparing Figs. 4 and 2, one can see that the early time behaviours of the drawdown and derivative are similar to the situation of Fig. 2a, indicating that the Theis solution must be applicable during that time period. Later, the derivative starts to decrease but the signal is not clear: some oscillations are visible in Fig. 4b; Fig. 4a even shows a noisy but important increase of the derivative.

This apparently erratic behaviour is a classic problem that can lead to wrong interpretations. Therefore, it must be well understood in order to avoid misinterpretations. It is an artefact due to the amplification of measurement errors. In Eq. 7, one can see that if the drawdown varies very slowly, then the difference between two successive drawdown values will be on the order of magnitude of the head measurement errors. These numbers can be positive and negative but remain bounded by the magnitude of the errors. The duration of the time interval in the denominator is often constant. However, as time passes the measurement errors are multiplied by increasing time values (Eq. 3), and are therefore amplified. Because the log–log plot cannot display the negative values, it shows only a misleading apparent increase of the derivative. Plotting the same data in semi-log scale (Fig. 4c) shows the stabilization of the drawdown and the amplification of the measurement errors around a zero mean derivative. The more robust way of computing the derivative that was explained earlier minimizes this effect and does not show such high oscillations and negative values (Figs. 4b and d).

In that example, the correct interpretation is therefore to observe that the drawdown is stabilizing at late time and

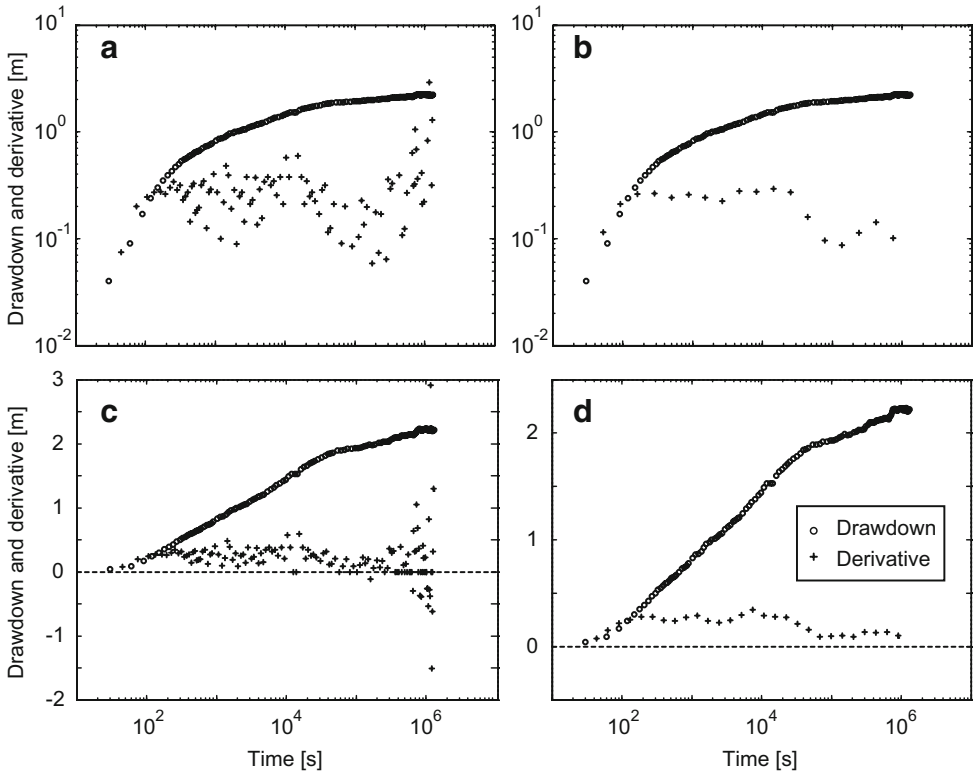

Fig. 4 Diagnostic plot of constant rate test in a coastal aquifer in Tunisia: **a** log–log scale, the derivative is calculated directly with Eq. (3); **b** log–log scale, the derivative is calculated with the sampling algorithm described in the text; **c** same as **a** in semi-log scale; **d** same as **b** in semi-log scale

that the derivative tends toward zero with strong oscillations. The typical diagnostic plots corresponding to this situation are therefore those of Fig. 2d,e or i. They show an initial behaviour similar to Theis and then a stabilization of the drawdown and a decrease of the derivative at late time. At least three models allow interpreting this behaviour: a leaky aquifer, an aquifer limited by a constant head boundary, or a spherical flow (flow dimension greater than 2). Here is an important aspect of well-test interpretation. Usually, there is not a unique model allowing one to describe the behaviour observed in the field. This non-uniqueness of interpretation needs to be resolved by integrating carefully the geological and hydrogeological knowledge available for the site. In this example, the most likely interpretation is the constant head boundary model because of the presence of the sea in the vicinity of the pumping well. To check if that interpretation is correct, a constant head model has been adjusted to the data, the distance to the boundary computed, and it was found that it was consistent with the real distance between the well and the sea. This confirmed the plausibility of the interpretation. More generally, when several interpretations are possible, evaluating the plausibility of the various interpretations by judging the plausibility of the parameters obtained during the interpretation is one possible way to reject some models. Combining observations from different piezometers is also a good way to eliminate some models that would not be coherent with all available information.

To conclude this section, it has been shown in detail that the derivative is very sensitive to measurement errors and can display artefacts that may be misleading in the interpretation. Techniques exist to reduce the problem but it cannot be completely avoided when working with real field data. Therefore the qualitative interpretation of the data must use the derivative as a general guide but it should never be overlooked. The shape of the derivative must be analyzed by looking simultaneously at the drawdown curve and its derivative. Only the main tendencies must be analysed, not the small variations which are often just noise. Using both the log–log and semi-log plots can help in the analysis.

A single well-test example

There are a number of cases in which the diagnostic plot makes a very significant difference in the interpretation. The following example illustrates one of these situations. The data are from a short term (46 min) pumping test in a large diameter well in a confined aquifer in South India (Fig. 4b of Rushton and Holt 1981). The semi-log plot of the data set is shown in Fig. 5.

On this graph, some inexperienced hydrogeologists would tend to draw a straight line for the late time data (Fig. 5) and estimate the transmissivity from the slope of the straight line. The slope of the straight line in Fig. 5 is

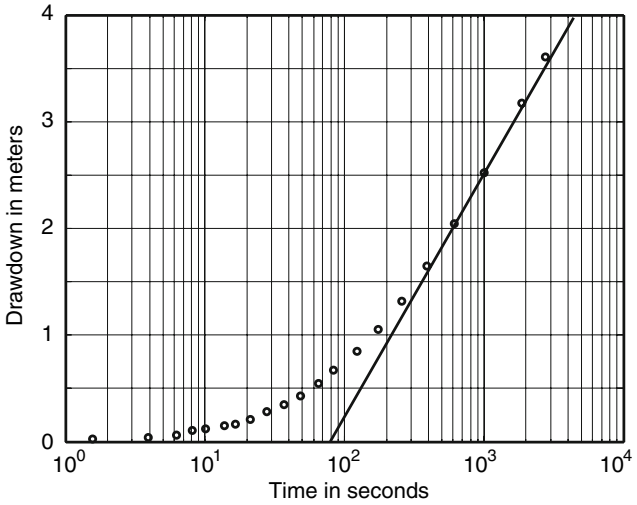

Fig. 5 Semi-log plot of pumping test data in a confined aquifer in South India, and a possible straight-line interpretation of late time data

2.25 m per log cycle. The corresponding transmissivity would then be:

$$T = \frac{0.183 \times 7.998\ 10^{-2}\left[m^3/s\right]}{2.25[m]} = 6.510^{-3}\left[m^2/s\right] \qquad (8)$$

This value is one order of magnitude larger than the value of 5.5 10^{-4} m^2/s that was estimated correctly by Rushton and Holt (1981) using a numerical model. Note that estimating numerically if the test lasted long enough to apply the Cooper-Jacob approximation is not trivial in that case. Being a single well test, it is known that the estimate of the storativity is not reliable due to potential quadratic head losses (Jacob 1947) in the well and skin effects (Agarwal et al. 1970). This example shows that the classical straight-line analysis applied rapidly can lead to highly incorrect results.

In the following, the same data are analyzed with a diagnostic plot in order to illustrate what is gained by the approach. Figure 6 shows the corresponding diagnostic plot; it has two important characteristics that are discussed in the next two sections.

Well-bore storage

First, during the early time, the drawdown and the derivative are roughly following the same straight line of unit slope, indicating that during all this period, the test is dominated by the well bore storage effect. During that period, it is not possible to estimate the transmissivity of the aquifer.

To understand why the derivative and the drawdown follow the same straight line in log–log scale, one can study the asymptotic case corresponding to a well that would be drilled in an aquifer having zero transmissivity. In that case, all the pumped water would come directly

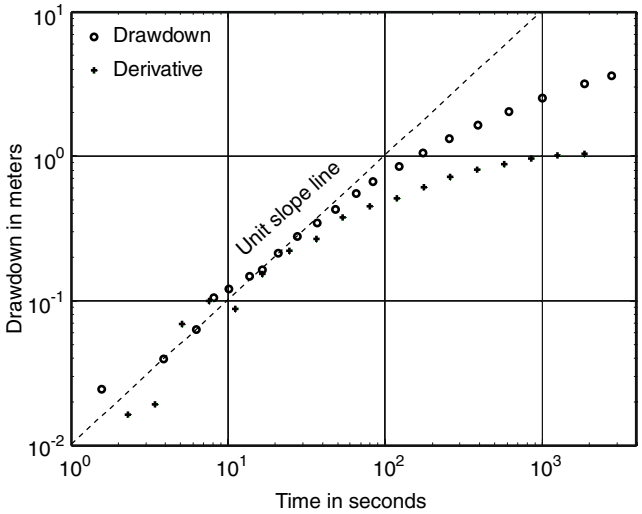

Fig. 6 Diagnostic plot of the same drawdown data as shown in Fig. 5

from the water stored in the well and the equation of the drawdown in the pumping well would be:

$$s(t) = \frac{Q}{\pi r_c^2} t \tag{9}$$

where Q [m^3/s] represents the pumping rate, t [s] the time, and r_c [m] the radius of the well casing. The calculation of the log derivative in that case shows that it is equal to the drawdown:

$$\frac{\partial s}{\partial \ln t} = t\frac{\partial s}{\partial t} = t\frac{Q}{\pi r_c^2} = s(t) \tag{10}$$

Furthermore, taking the logarithm of this expression shows that both the logarithm of the derivative and the logarithm of drawdown are the same linear function of the logarithm of the time. This linear function has a unit slope:

$$\log[s(t)] = \log\left[\frac{\partial s}{\partial \ln t}\right] = \log(t) + \log\left[\frac{Q}{\pi r_c^2}\right] \tag{11}$$

In summary, these asymptotic equations show that well-bore storage is characterized at early time by a unit-slope straight line in log–log scale both for the drawdown and its log derivative. This behaviour has to be expected in most cases when drawdown is observed in a pumping well.

Infinite acting radial flow (IARF)

The second important characteristic visible on Fig. 6 is that the derivative does not stabilize: it increases during the entire the duration of the test. Why is this important? In the first example, it was shown that the Cooper-Jacob approximation can be applied when the derivative stabilizes in an observation well. When analyzing data from the pumping well itself, one has to account in addition for well-bore storage, quadratic head losses and skin effect. However, the important point is that the solution that accounts for all these effects tend asymptotically toward the Cooper and Jacob (1946) asymptote plus two time-independent terms related to skin factor σ [–] and quadratic head losses coefficient B [s^2/m^5] (Kruseman and de Ridder 1994):

$$s(t) = \frac{Q}{4\pi T}\ln\left(\frac{2.25tT}{r^2S}\right) + \frac{Q}{2\pi T}\sigma + BQ^2 \tag{12}$$

Equation (12) implies that the logarithmic derivative of the drawdown tends toward a constant value at late time independent of the well-bore storage, quadratic head losses, and skin effect (compare with Eq. 2).

$$\frac{\partial s}{\partial \ln t} = t\frac{\partial s}{\partial t} = t\frac{Q}{4\pi T}\frac{1}{t} = \frac{Q}{4\pi T} \tag{13}$$

Therefore, in a similar manner where one can not apply the Cooper-Jacob approximation to estimate the transmissivity when the derivative is not constant in the data collected in an observation well, one can not apply Eq. (12) if the derivative is not constant in the data collected in the pumping well. The diagnostic plot (Fig. 6) does not show any stabilization of the derivative and therefore the straight-line analysis presented in Fig. 5 was wrong because the IARF period was not reached.

Synthesis for this example

The diagnostic plot (Fig. 6) allows for very clear identification of the well bore storage effect that occurs during the early stage of the test. By comparing it with the typical diagnostic plots (Fig. 2), it shows that one has to use a model that includes well-bore storage and skin effect to interpret quantitatively those data. The comparison also shows that the data correspond only to the early part of the typical diagnostic plot. There is no clear stabilization of the derivative and therefore a straight-line analysis cannot be used. The quantitative interpretation requires one then to use the complete analytical solution of Papadopulos and Cooper (1967) for a large diameter well or those of Agarwal et al. (1970), which accounts in addition for skin effect. A non-linear fit of the analytical solution to the complete data set allows one then to estimate a value of 5.5 10^{-4} m^2/s for the transmissivity (Fig. 7) identical to those estimated earlier by Rushton and Holt (1981). The plot of the model drawdown and model derivative (Fig. 7) allows a graphical check to ensure that the model fits well the observation.

The situation described in this example is classic: the test was terminated too early. The IARF period was not reached, and most of the data are affected by the well-bore storage effect masking the response of the aquifer. The

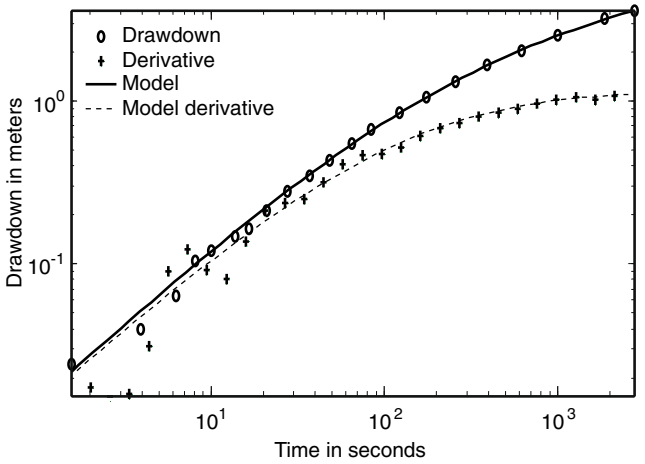

Fig. 7 Quantitative interpretation of the data from Rushton and Holt (1981)

slight departure from the straight line allows estimation of the transmissivity, but it is not sufficient to identify without doubt the type of aquifer response or any boundary effect. It is impossible to obtain reliable estimates of the aquifer properties with straight-line analysis. To avoid such a situation, it is recommended (e.g. Ehlig-Economides et al. 1994a) to use real-time on site computation of the diagnostic plot to check that the test lasted long enough to achieve its objective and decide when the test can really be stopped. This is particularly important when testing, for example, low permeability formations using single well tests.

The most typical diagnostic plots

It is now important to come back to the theory and summarize what are the most typical features that are observable in diagnostic plots and that must be understood from a qualitative point of view to recognize them when analyzing field data. Those features are displayed in Fig. 2.

Figure 2a shows the diagnostic plot of the Theis solution. The typical characteristics of this solution are that the derivate stabilizes at late time indicating an infinite acting radial flow (IARF) period, and that the derivative is larger than the drawdown at early time. Figure 2f shows the diagnostic plot for the Papadopulos-Cooper solution for a large diameter well, which was discussed in the previous section. It shows a stabilization of the derivative at late time corresponding to the infinite acting radial flow period. The early time behaviour is characterized by a unit slope straight line in log–log scale. During intermediate times, the derivative makes a hump. The size of this hump varies as a function of the duration of the well bore storage effect. For a very large diameter well, the hump will be more pronounced than for a small diameter well. In addition, Agarwal et al. (1970) have shown that exactly the same shape of diagnostic plots occurs when a skin effect reduces the transmissivity of a narrow zone around the pumping well. In that case, the duration of the unit slope straight-line period and the size of the hump are a function of the combined skin and well-bore storage effects.

Figure 2b shows another typical behaviour—an inflection of the drawdown at intermediate time that is reflected by a pronounced hole in the derivative. This is a behaviour that can be modelled by a delayed yield and is typical of double porosity, double permeability and unconfined aquifers. The process that leads to this behaviour is one in which the early pumping depletes a first reservoir that is the well connected to the pumping well (the fractures for example, or the saturated zone of an unconfined aquifer). The depletion in this reservoir is then partly compensated for by a delayed flux provided by a second compartment of the aquifer. It can either be the vertical delayed drainage of the unsaturated zone above the saturated part in an unconfined aquifer (Moench 1995; Neuman 1972) or the drainage of matrix blocks in fractured (Warren and Root 1963) or karstic (Greene et al. 1999) aquifers. During that period, the drawdown stabilizes and the derivative shows a pronounced hole. At late time, the whole system equilibrates and behaves as an equivalent continuous medium that tends toward a Cooper-Jacob asymptote (IARF).

Figure 2c,d shows the effect of an infinite linear boundary. A no-flow boundary is characterized by a doubling of the value of the derivative, while a constant head boundary (Theis 1941) is characterized by a stabilization of the drawdown and a linear decrease of the derivative.

It is interesting to observe that, at least in theory, the case of a leaky aquifer (Hantush 1956) can be distinguished from the case of the constant head boundary when looking at the shape of the derivative (Fig. 2e). Here, the derivative tends toward zero much faster than the constant head case.

The case of a vertical fracture of finite extension but infinite conductivity (Gringarten et al. 1974) is shown in Fig. 2g. It is characterized by an early period in which the effect of the fracture dominates and a constant difference between the derivative and the drawdown corresponding to a multiplying factor of 2. After a transition period, the solution tends toward a late time Cooper-Jacob asymptote with a stabilization of the derivative (IARF).

Flow dimensions different than 2 are modelled with the general radial flow model (Barker 1988) and are characterized by a derivative which is behaving linearly at late time in the diagnostic plot. The slope m of the derivative allows one to infer the flow dimension n (Chakrabarty 1994):

$$m = 1 - \frac{n}{2} \tag{14}$$

This is what is shown in Fig. 2h and i, corresponding respectively to a flow dimension n lower than 2 (positive slope) or higher than 2 (negative slope). In this framework, a spherical flow (n=3) is characterized by a slope of

the derivative of –1/2, a linear flow (n=1) is characterized by a slope of the derivative of 1/2. Non-integer flow dimensions (whether fractal or not) are characterized by intermediate slopes.

This catalogue of diagnostic plots could be extended to many other cases (Bourdet 2002), but a very important aspect that needs to be discussed here is that all the typical behaviours can occur during shorter or longer periods as a function of the values of the physical parameters that control them. Sometimes they are extremely clear, sometimes they are partly masked and much more difficult to identify. Furthermore, the exact shape of the diagnostic plot depends on the value of the various parameters that control the analytical solution. For example, the effect of a boundary will be visible at a different time depending on the position of the observation well with respect to the boundary. The depth of the hole in the derivative for a double porosity model will depend on the relative properties of the matrix and the fractures. Therefore all the curves shown in Fig. 2 are only indicative of a certain family of response and not strictly identical to a single response that one should expect in the reality. In addition, the different behaviours are usually combined as illustrated in Fig. 2j, where the early time shows a well-bore storage effect followed by an infinite acting radial flow period which is then followed by a constant head boundary.

Therefore, the interpretation of a diagnostic plot is usually conducted by analyzing separately the different phases of the test data. The early data allow for identification if well bore storage is present. Intermediate time data are analyzed to identify the type of aquifer model that should be used (two-dimensional confined, double porosity, unconfined, non-integer flow dimension, etc.) and then the late time data allow for identification of the presence of boundaries.

Along this line of thought, a practical tool is the flow-regime identification tool (Ehlig-Economides et al. 1994b). It is a diagram (Fig. 8) that shows in a synthetic way the behaviour of the derivative as a function of the main type of flow behaviour. The diagram can be superposed to the data and shifted to identify visually and rapidly the type of flow that occurs during a certain period of the test. Several examples of the use of this tool are provided in the paper of Ehlig-Economides et al. (1994b).

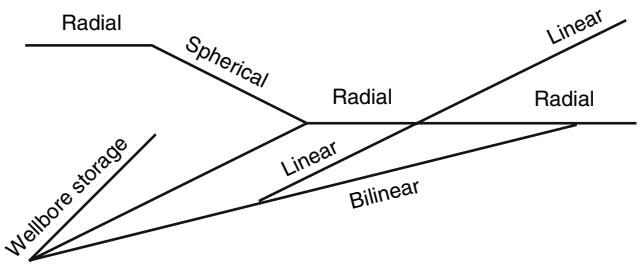

Fig. 8 Flow regime identification tool representing schematically the log-derivative of drawdown as a function of logarithmic time (redrawn from Ehlig-Economides et al. 1994b)

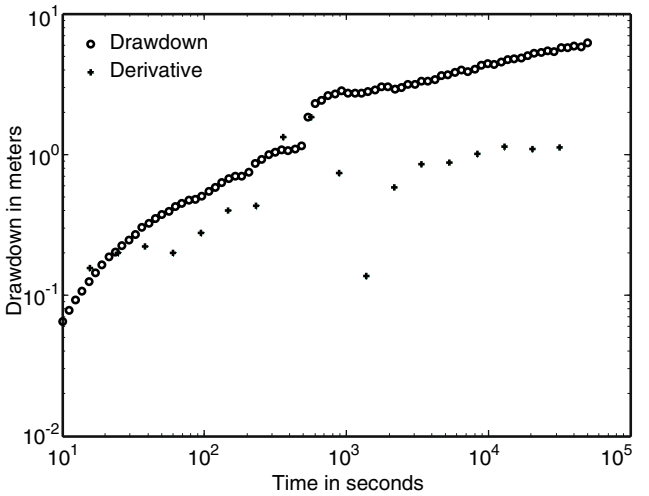

Fig. 9 Typical diagnostic plot obtained from a data set in which the pumping rate could not be maintained constant

Variable rate tests

The diagnostic plots described in the previous section are based on analytical solutions that assume a constant pumping rate. However, the pumping rates are often variable in practice, which can be due to practical difficulties, or it can be made variable on purpose to evaluate the well performances with a step-drawdown test. In those cases, the diagnostic plot of the raw data will probably look like Fig. 9. This is a synthetic example that was built by computing the response of an aquifer from an observation well and adding random noise to the calculated drawdowns. There are six consecutive small and larger variations of pumping rate of different durations during the test. The results (Fig. 9) show sudden variations in drawdown that are amplified in the diagnostic plot and which are not interpretable directly.

One solution to continue to use the diagnostic plot is to use a deconvolution algorithm such as the one proposed by Birsoy and Summers (1980) for a series of successive constant rate tests. The deconvolution technique uses the superposition principle to extract the theoretical response of the aquifer if the pumping rate had been kept constant and equal to unity using the variable rate test data.

If the pumping-rate variations are a series of constant steps, the technique of Birsoy and Summers consists of computing the equivalent time t_b and specific drawdown s_b values for every data point. The formulae can be found in the original paper (Birsoy and Summers 1980) and several books (e.g. Kruseman and de Ridder 1994) and are simple to program with any spreadsheet. If the flow rates vary continuously in time, other more sophisticated algorithms are required (e.g. Levitan 2005; von Schroeter et al. 2001).

In the example presented here, the diagnostic plot of the deconvoluted signal is shown in Fig. 10, which shows the hole in the derivative corresponding to the inflection of the drawdown curve that is characteristic of a double

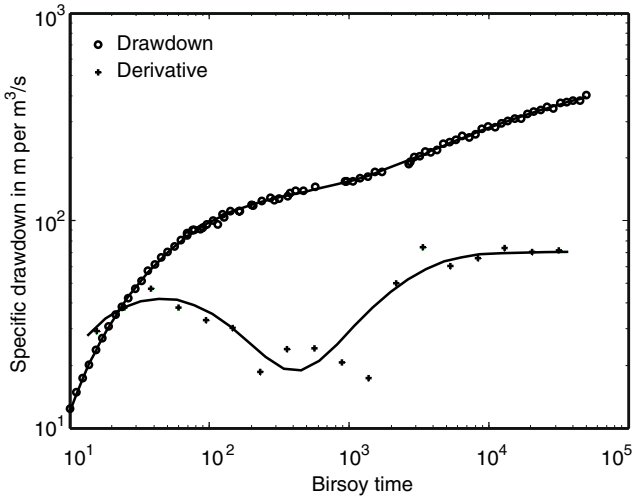

Fig. 10 The same data as Fig. 9, but the diagnostic plot is made after deconvolution of the data using the formulas of Birsoy and Summers (1980). A double porosity model has been adjusted to the data

porosity model and was completely impossible to identify on Fig. 8. One can then go a step further and adjust a double porosity model on those deconvoluted data in a similar way to Birsoy and Summers, who were adjusting a Cooper-Jacob straight line to the deconvoluted data that they were presenting in their original article.

To summarize, this example shows that even when the flow rates are not constant, it is still possible to use the standard technique of a diagnostic plot. However it requires that the principle of superposition can be applied to use the deconvolution technique (it may not work for unconfined aquifer with, for example, too strong head variations). It also requires that the variations of the pumping rate are known with enough accuracy and this is often one of the major difficulties in real field applications.

Similarly, the recovery after a pumping period can be interpreted with the help of diagnostic plots like the pumping period using the equivalent Agarwal time (Agarwal 1980). For a constant rate test prior to the recovery, the expression of the Agarwal time is the following:

$$t_a = \frac{t_p t_r}{t_p + t_r} \tag{15}$$

where t_p is the duration of the pumping, and t_r the time since the start of the recovery. For a variable rate test prior to the recovery, Agarwal (1980) provides as well an expression that can be used to interpret the recovery with diagnostic plots.

Time shift

This section describes the impact of time shift, which is an important issue because this type of error influences the shape of the diagnostic plots and may induce misinterpretations. Time shift occurs when the time at which the pumping started is not known accurately; it can occur for example because the clocks of different data acquisition systems (data loggers) on a site are not synchronized properly, or if the real start time of the pump is not noted properly (when the time interval between two head measurements is large). It can also occur when a pump did not start instantaneously when it is powered on, which leads to an uncertainty in the elapsed time t, which may be underestimated or overestimated by a certain constant—the time shift.

$$t = t_{true} + t_{shift} \tag{16}$$

To illustrate the consequences of a possible time shift, one can take the data from the short-term pumping test of Rushton and Holt (1981) and add an artificial error to the time values. The correct diagnostic plot was presented in Fig. 6. When a negative time shift of 20 s is imposed (the pump is assumed to have started 20 s earlier than it really started), the diagnostic plot (Fig. 11a) does not show anymore the wellbore storage effect, but rather an

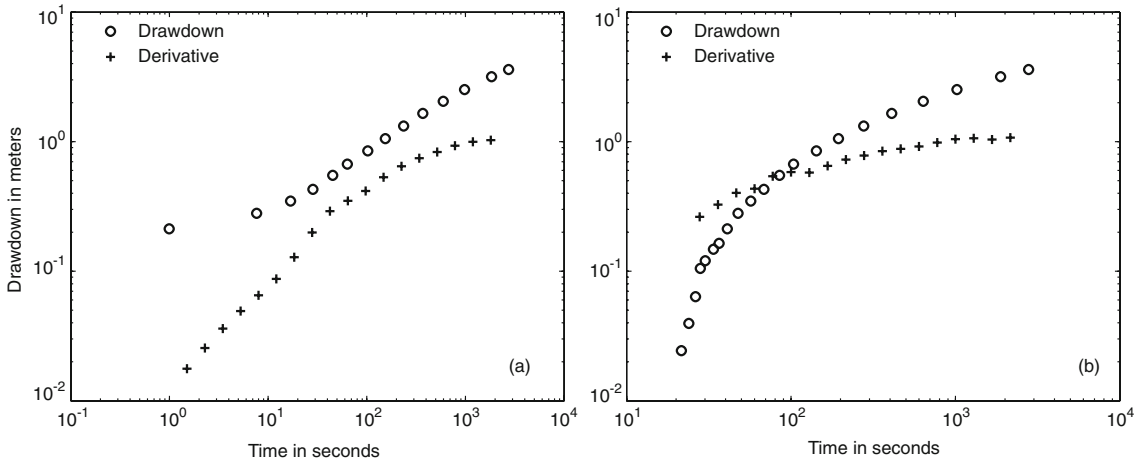

Fig. 11 Impact of a time shift on a diagnostic plot. The data are the same as in Fig. 7: **a** time shift of –20 s; **b** time shift of +20 s

inflection that may incorrectly be attributed to a delayed yield. When a positive time shift of 20 s is imposed (the pump is assumed to have started 20 s later than it really started), the effect is again that the wellbore storage effect is hidden and the diagnostic resembles a standard Theis curve (Fig. 11b).This problem can be avoided with rigorous procedures during field data acquisition, but it is important to know its existence when interpreting data that may not have a high temporal accuracy.

Finally, when a time shift is suspected and when it is compatible with possible time-measurement errors due to field procedures, the approach involves correcting the measured time in order to obtain a meaningful diagnostic plot. For a single well test, in which a unit slope line is expected at the beginning, the procedure consists of correcting the time until the diagnostic plot shows a unit slope line at early time. This can be more difficult for interference tests, emphasizing again the need for accurate data acquisition.

Conclusions

Diagnostic plots can be used to enhance and facilitate the interpretation of well-test data. One of the main advantages is that the techniques allows for identification of certain flow regimes and facilitates the selection of an appropriate model. The general procedure to use diagnostic plots is straightforward:

- The logarithmic derivative of the drawdown is calculated and plotted together with the drawdown data on a bi-logarithmic plot.
- This diagnostic plot is analyzed in a qualitative manner by comparing it with a catalogue of typical diagnostic plots. It allows for identification of a set of model candidates that may be able to explain the observed data. Some model candidates are eliminated based on geological judgement.
- The remaining models are used following a rather classic approach which consists of fitting the model to the data in order to obtain the values of the model parameters (physical parameters) that allow the data (drawdown and derivative) to be reproduced as accurately as possible.

This procedure shows that diagnostic plots are not a substitute for the classic approach but rather a flexible complement that should help the hydrogeologist decide between different possible alternatives during the interpretation process.

Because of its high sensitivity to small variations in the drawdown and time values, the diagnostic plot has to be used carefully. Artefacts in the shape of the derivative occur with inaccurate and noisy data. Some techniques minimize these effects but, in order to ensure the best quality of the interpretation, the data acquisition must be performed with care. The accuracy of the measurements should be as high as possible. When using pressure sensors, particular attention must be devoted to the selection of the sensors which will provide the best accuracy in the range of expected drawdown and avoid saturation effects. The flow rates must be recorded regularly and accurately. The natural variations of the groundwater level (independent of pumping) must be monitored to be able to detrend the data.

While these problems are real, it is important to remember that they are not specific to the use of the diagnostic plot. They also influence the traditional interpretation techniques. The main difference is that often, when traditional techniques are used, it is not easy to visualize whether the interpretation is valid or not. The diagnostic plot makes the problems more visible. Finally, diagnostic plots cannot resolve the non-unicity problems inherent in the inverse nature of well-test interpretation, which means that interpretation will always require a critical examination of the local geology and flow conditions in order to provide meaningful results.

Acknowledgements The authors thank R. Beauheim, P. Hsieh and an anonymous reviewer for their constructive comments which helped to improve the manuscript. The work was conducted within a joint research project funded by the Geological Survey of Spain and the University of Neuchâtel. Philippe Renard was supported by the Swiss National Science Foundation (grant PP002–1065557).

References

Agarwal RG (1980) A new method to account for producing time effects when drawdown type curves are used to analyze pressure buildup and other test data. Paper presented at the 55th Annual Fall Technical Conference and Exhibition of the Society of Petroleum Engineers of AIME, Dallas, TX, 21–24 September 1980

Agarwal RG, Al-Hussainy R, Ramey HJJ (1970) An investigation of wellbore storage and skin effect in unsteady liquid flow. 1. Analytical treatment. SPE J 10:279–290

Bardsley WE, Sneyd AD, Hill PDH (1985) An improved method of least-squares parameter estimation with pumping-test data. J Hydrol 80:271–281

Barker JA (1988) A generalized radial flow model for hydraulic tests in fractured rock. Water Resour Res 24:1796–1804

Beauheim RL, Roberts RM, Avis JD (2004) Well testing in fractured media: flow dimensions and diagnostic plots. J Hydraul Res 42:69–76

Birsoy YK, Summers WK (1980) Determination of aquifer parameters from step tests and intermittent pumping data. Ground Water 18:137–146

Bourdet D (2002) Well test analysis. Elsevier, Amsterdam

Bourdet D, Whittle TM, Douglas AA, Pirard YM (1983) A new set of type curves simplifies well test analysis. World Oil 196:95–106

Bourdet D, Ayoub JA, Pirard YM (1989) Use of pressure derivative in well-test interpretation. SPE Reprint Ser 4:293–302

Chakrabarty C (1994) A note on fractional dimension analysis of constant rate interference tests. Water Resour Res 30:2339–2341

Chow VT (1952) On the determination of transmissibility and storage coefficients from pumping test data. Trans Am Geophys Union 33:397–404

Cooper HHJ, Jacob CE (1946) A generalized graphical method for evaluating formation constants and summarizing well field history. Trans Am Geophys Union 27:526–534

Dawson KJ, Istok JD (1991) Aquifer testing. Lewis, Boca Rataon, FL

Delay F, Porel G, Bernard S (2004) Analytical 2D model to invert hydraulic pumping tests in fractured rocks with fractal behavior. Water Resour Res 31, L16501. doi:10.1029/2004GL020500
Ehlig-Economides CA, Hegeman P, Clark G (1994a) Three key elements necessary for successful testing. Oil Gas J 92:84–93
Ehlig-Economides CA, Hegeman P, Vik S (1994b) Guidelines simplify well test analysis. Oil Gas J 92:33–40
Fetter CW (2001) Applied hydrogeology, 4th edn. Prentice Hall, Upper Saddle River, NJ
Greene EA, Shapiro AM, Carter JM (1999) Hydrogeological characterization of the Minnelusa and Madison aquifers near Spearfish, South Dakota. US Geol Surv Water Resour Invest Rep 98-4156, pp. 64
Gringarten A, Ramey HJJ, Raghavan R (1974) Unsteady-state pressure distributions created by a single infinite conductivity vertical fracture. Soc Petrol Eng J 14:347
Hamm S-Y, Bideaux P (1996) Dual-porosity fractal models for transient flow analysis in fractured rocks. Water Resour Res 32:2733–2745
Hantush MS (1956) Analysis of data from pumping test in leaky aquifers. Trans Am Geophys Union 37:702–714
Horne RN (1994) Advances in computer-aided well-test interpretation. J Petrol Technol 46:599–606
Horne R (1995) Modern well test analysis, 2nd edn. Petroway, Palo Alto, CA
Jacob CE (1947) Drawdown test to determine effective radius of artesian well. Trans Am Soc Civ Eng 112:1047–1064
Kruseman GP, de Ridder NA (1994) Analysis and evaluation of pumping test data. ILRI, Nairobi, Kenya
Levitan MM (2005) Practical application of pressure/rate deconvolution to analysis of real well tests. SPE Reserv Eval Eng 8:113–121
Moench AF (1995) Combining the Neuman and Boulton models for flow to a well in an unconfined aquifer. Ground Water 33: 378–384
Neuman SP (1972) Theory of flow in unconfined aquifers considering delay response of the watertable. Water Resour Res 8:1031–1045
Papadopulos IS, Cooper HHJ (1967) Drawdown in a well of large diameter. Water Resour Res 3:241–244
Ramey HJJ (1992) Advances in practical well-test analysis. J Petrol Technol 44:650–659
Renard P (2005a) The future of hydraulic tests. Hydrogeol J 13:259–262
Renard P (2005b) Hydraulics of well and well testing. In: Anderson MG (ed) Encyclopedia of hydrological sciences. Wiley, New York, pp 2323–2340
Rushton KR, Holt SM (1981) Estimating aquifer parameters for large-diameter wells. Ground Water 19:505–509
Spane FA, Wurstner SK (1993) DERIV: a computer program for calculating pressure derivatives for use in hydraulic test analysis. Ground Water 31:814–822
Theis CV (1935) The relation between the lowering of the piezometric surface and the rate and duration of discharge of a well using groundwater storage. Trans Am Geophys Union 2:519–524
Theis CV (1941) The effect of a well on the flow of a nearby stream. Trans Am Geophys Union 22:734–738
Toll NJ, Rasmussen TC (2007) Removal of barometric pressure effects and earth tides from observed water levels. Ground Water 45:101–105
Veneruso AF, Spath J (2006) A digital pressure derivative technique for pressure transient well testing and reservoir characterization. Paper presented at the 2006 SPE Annual Technical Conference and Exhibition, San Antonio, TX, 24–27 September 2006
von Schroeter T, Hollaender F, Gringarten A (2001) Deconvolution of well test data as a nonlinear total least squares problem. Paper presented at the 2001 SPE Annual Technical Conference and Exhibition, New Orleans, LA, 30 September–3 October 2001
Warren JE, Root PJ (1963) The behaviour of naturally fractured reservoirs. Soc Petrol Eng J 3:245–255